https://doi.org/10.15407/ujpe63.2.182

N. GEMECHU, T. ABEBE

Jimma University, Department of Physics
*(P.O. Box 378, Jimma, Ethiopia; e-mail: nebgem.eyu@gmail.com)*

# STRUCTURAL CHARACTERIZATION AND THICKNESS PROFILE OF PULSED LASER-DEPOSITED $KY_3F_{10} : Ho^{3+}$ THIN FILMS

*Thin films of $KY_3F_{10} : Ho^{3+}$ have been successfully prepared by the pulsed laser deposition with a Nd-YAG laser (266 nm, pulse duration of 10 ns, repetition rate of 2 Hz) on a 1 cm × 1 cm silicon substrate in vacuum and for different target-to-substrate distances. The X-ray diffraction (XRD) results show that the films crystallized in the tetragonal polycrystalline phase of $KY_3F_{10}$ (in agreement with JCPDS card No. 27-0465). Theoretical predictions of the thickness profile have been presented, by using some experimental parameters used in the deposition. Assuming the ellipsoidal expansion of the plasma plume, the thickness profiles of films have been estimated from the solution of the gas dynamical equations for the adiabatic expansion of the plasma plume into vacuum. The results show the strong forward direction of the plume and are in a good agreement with experimental results. Both theoretical and experimental results show a decrease in the film thickness for relatively larger values of the target-to-substrate distance, and this could be attributed to a decrease in the deposition rate at such larger distances. Moreover, for a single film, the thickness also decreases for relatively larger radial angles with respect to the normal to the substrate.*

*Keywords*: thickness profile, gas dynamic equations, plasma plume.

## 1. Introduction

Pulsed laser deposition (PLD) is a thin film deposition technique, which has been a popular, versatile, and highly flexible method for the thin film growth for various materials [1–3]. Using this technique, the advantage of controlling a thin film stoichiometry accurately can be achieved by controlling the deposition parameters. The expansion of a laser-induced plasma plume increases on its way from the target to the substrate. This varies the particle flux of the target species over the substrate area, which makes the different parts of the same film to have slightly different thicknesses. It is reported that, near the axis of the plasma plume, the angular distribution of the flux species is proportional to $\cos^n\theta$, where $n \gg 1$ and $\theta$ is the radial angle with respect to the normal to the substrate [4]. The cause for this strong forward direction is the strong differences in pressure gradients in axial and radial directions. R.K. Singh and J. Narayan investigated the problem of the angular distribution of the mass flow in the plasma expansion, by using the isothermal solution of the following gas dynamical equations with Gaussian pressure and density profiles [5]:

$$\frac{\partial \rho}{\partial t} + \mathrm{div}(\rho\nu) = 0, \tag{1}$$

$$\frac{\partial \nu}{\partial t} + (\nu \cdot \boldsymbol{\nabla})\nu + \frac{1}{\rho}\nabla P = 0, \tag{2}$$

$$\frac{\partial S}{\partial t} + (\nu \cdot \boldsymbol{\nabla})S = 0, \tag{3}$$

where $\rho$, $P$, $\nu$, and $S$ are the density, pressure, velocity, and entropy, respectively. However, since there exists a considerable temperature gradient inside the plasma plume [4, 6], the consideration of isothermal solutions is inadequate for the description of PLD. S.I. Anisimov *et al.* considered the adiabatic expansion of a plume, which is a more realistic situation [4] and described the ellipsoidal expansion of a plasma plume in to vacuum by the above gas dynamic equations as well. By assuming that the evaporated material can be described by the equation of ideal gases with a constant adiabatic exponent $\gamma = c_p/c_\nu$, they rigorously derived the angular dependence of the

film thickness $h(\theta)$, which is given by

$$h(\theta) = \frac{Mk^2}{2\pi\rho_s d_{ts}^2}(1 + k^2\tan^2\theta)^{-3/2}, \quad (4)$$

where $M$ is the plume mass, $\rho_s$ is the density of the deposited material, $k$ is a constant, and $\theta$ is as defined above. This is a powerful technique in determining the thickness profile of a deposited film theoretically. The target-to-substrate distance ($d_{ts}$) is one of the most critical factors, which affect the quality of films in PLD. A variation in $d_{ts}$ changes the value of the radial angle $\theta$ (from simple trigonometry) and the thickness profile $h(\theta)$. It is clear that the thickness profile depends both on $d_{ts}$ and $\theta$. In this work, the thickness profiles of films deposited at various $d_{ts}$ are presented, by using some experimental values. The theoretical and experimental results are then compared. Figure 1 depicts the typical expansion of a plasma plume and the deposition of a film. The parameters $x_0$ and $R_0$ are the initial height and radius of the plasma plume, respectively. Here, $R_0$ can be approximated by the laser spot radius.

## 2. Experimental Details

The preparation of $KY_3F_{10}:Ho^{3+}$ thin films was carried out, by using a Nd-YAG laser (266 nm, pulse duration of 10 ns, and repetition rate of 2 Hz). The laser fluence was kept at 1.2 J/cm$^2$. The radius of the laser spot was 0.5 mm. The vacuum chamber was evacuated to a background pressure of $4 \times 10^{-5}$ mbar. The films were grown at different target-to-substrate distances equal to 4, 5 and 6.7 cm on the 1 cm × 1 cm (100) silicon substrate. The substrate temperature was kept at 600 °C. The targets were made of a commercially obtained $KY_3F_{10}:Ho^{3+}$ powder pressed into pellets. The crystal structure of the films was analyzed by X-ray diffraction (XRD), by using a Bruker D8 advance X-ray diffractometer operating at 40 kV and 40 mA with the use of the Cu$K\alpha$ emission at 0.15406 nm. The thicknesses of the films were estimated, by using the weight difference method employing a sensitive electronic microbalance.

## 3. Results and Discussion

Figure 2 illustrates the XRD pattern of films deposited at different target-to-substrate distances for a constant deposition temperature of 600 °C in vacuum. The Miller indices of the prominent peaks are

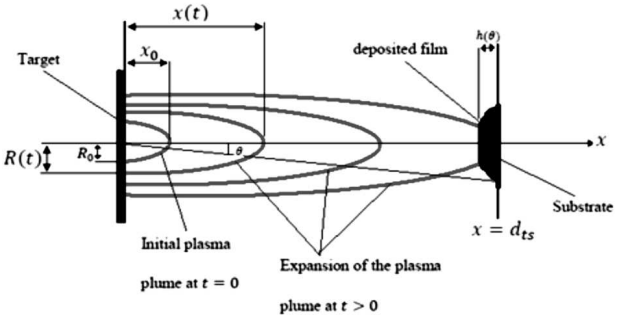


***Fig. 1.*** Elliptical plasma plume expansion and the deposited film. $R_0$ and $x_0$ are the initial parameters of the plume at $t = 0$. $R(t)$ and $x(t)$ are the final radius and height of the plume at $t > 0$. The ablated material is deposited and forms a thin film with the thickness profile $h(\theta)$ after reaching $x = d_{ts}$

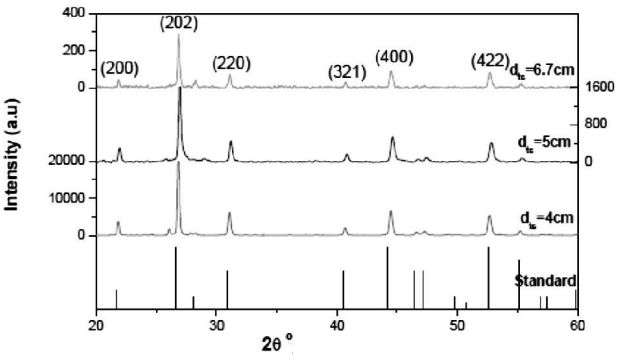


***Fig. 2.*** XRD pattern of $KY_3F_{10}:Ho^{3+}$ thin films prepared at different target-to-substrate distances. The standard is included for comparison

shown. This result indicates that the films crystallized in the tetragonal structure of $KY_3F_{10}$ (in agreement with JCPDS card No. 27-0465). The film deposited at $d_{ts} = 4$ cm has relatively the highest diffraction peaks among all samples, suggesting that the better crystalline quality was obtained at this particular value of $d_{ts}$. The change in the degree of crystallinity of the films is presented in terms of the actual surface temperature of the films, which depends on two factors. The first factor is the substrate heating by a heater, and the second factor is the kinetic energy of the vapor species striking the surface [7]. Since the substrate heating by a heater is kept constant at 600 °C, the second factor might have influenced the structure of the films.

The average crystallite size has been computed from the full width at half maximum (FWHM) of the dominant peaks, by using Scherrer's formula, which

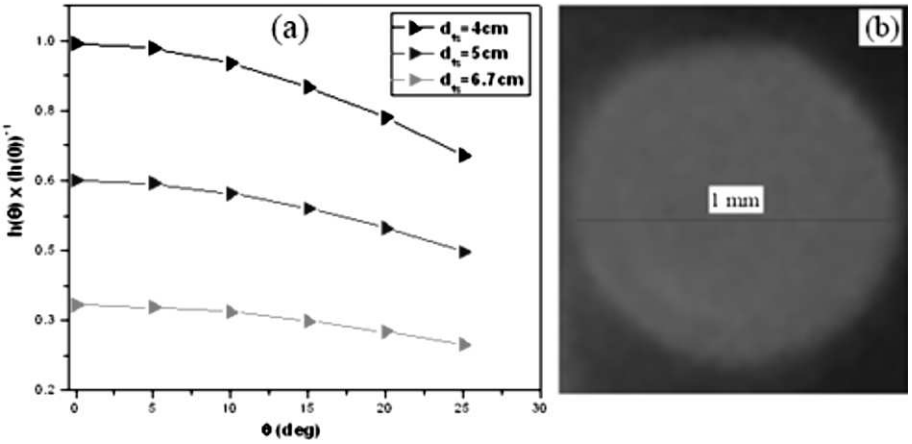


***Fig. 3.*** Stationary thickness profile of the films deposited for $k = 1$ and various values of $d_{ts}$ ($a$), and the micrograph of a single shot laser burnt spot ($b$). The diameter of the spot is about 1 mm

is given by [8]

$$D = \frac{0.9\lambda}{\beta \cos\theta}, \tag{5}$$

where $D$ is the crystallite size, $\lambda$ is the X-ray wavelength (0.15406 nm), $\beta$ is the FWHM, and $\theta$ is the diffraction angle. The average crystallite size of the films varied between 30.2 and 40 nm.

At lower values of $d_{ts}$, fewer collisions occur within the plasma and the target species strike the substrate with a relatively high kinetic energy. In other words, the vapor species travelling for relatively larger distances will make a higher number of collisions with the background gas molecules and, hence, have a lower kinetic energy, when reaching the substrate, as compared to the species travelling for shorter distances. Therefore, the substrate located at $d_{ts} = 4$ cm has the highest actual surface temperature and the adatom mobility resulting in the improved crystallinity with increased crystallite size as compared to those located at $d_{ts} = 5$ and 6.7 cm. The increment in FWHM at $d_{ts} = 5$ and 6.7 cm compared to its value at $d_{ts} = 4$ cm indicates a decrease in the crystallinity with rise in $d_{ts}$. In general, the crystallinity and FWHM are reported to have an inverse relation [9–10].

Quantitative information concerning the preferential crystallite orientation was obtained from the texture coefficient ($TC(hkl)$). It represents the texture of a particular plane, and its deviation from unity implies a preferred growth. ($TC(hkl)$) is defined as [11–12]

$$TC(hkl) = \frac{I(hkl)/I_0(hkl)}{N^{-1}\Sigma_N(I(hkl)/I_0(hkl))}, \tag{6}$$

where $I(hkl)$ is the measured intensity of the (($hkl$) diffraction peak, $I_0(hkl)$ is the standard intensity of JCPDS, and $N$ is the total number of diffraction peaks considered in the analysis. The value of $TC(202)$ for the (202) peak of all the films is greater than unity, by indicating the preferential growth of $KY_3F_{10} : Ho^{3+}$ crystal along the $C$-axis.

The film thickness ($t$) is also an important parameter in the study of film properties. The thicknesses of the films were estimated, by using the weight difference method employing a sensitive electronic microbalance and is given by [13]

$$t = \frac{m_2 - m_1}{\rho A}, \tag{7}$$

where $m_1$ and $m_2$ are, respectively, the masses of the substrate before and after the deposition, $\rho$ is the density of the film material ($g$ cm$^{-3}$), and $A$ is the area of the film (cm$^2$). The evaluated film thicknesses are $t = 752$, 627 and 483 nm for $d_{ts} = 4$, 5 and 6.7 cm, respectively.

The thickness profile of the films theoretically obtained with the use of Eq. (2) is shown in Fig. 3, $a$ with $k = 1$ and $h(0) = M(2\pi\rho_s)^{-1}$. The observed reasonable variation of $\theta$ within the context of the size of the substrate used is from 0 to 25°. It is clear that,

**Film thickness, average crystallite size, and FWHM for the dominant (202) peak**

| $d_{ts}$ (cm) | Film thickness (nm) | Average crystallite size (nm) | FWHM (for the dominant (202) peak) in degrees |
|---|---|---|---|
| 4 | 752 | 40 | 0.17417 |
| 5 | 627 | 37 | 0.18439 |
| 6.7 | 483 | 30 | 0.23432 |

in addition to the angular variation of the thickness of a single film, the relative thickness of the films decreased with increasing $d_{ts}$. The general trend of the decrease in the thickness of the films is in a good agreement with the experimental results. In both theoretical and experimental approaches, a decrease in the film thickness for relatively larger values of $d_{ts}$ could be attributed to a decrease in the deposition rate at such larger distances. The expansion of the laser-induced plasma plume increases with $d_{ts}$. This reduces the particle flux of the target species over the substrate area, which lowers the deposition rate and the thickness [14]. Moreover, for a single film, the particle flux reaching the substrate also decreases with increasing the radial angle $\theta$ with respect to the normal to the substrate. This is the reason why the thickness of the films decreases for relatively larger values of $\theta$.

## 4. Conclusion

The structure and thickness profile of $KY_3F_{10}:Ho^{3+}$ thin films is investigated. The films crystallized in the tetragonal polycrystalline phase of $KY_3F_{10}$ (in agreement with JCPDS card No. 27-0465). The value of $TC(202)$ for the (202) peak of all the films is greater than unity indicating the strong preferential growth of a $KY_3F_{10}:Ho^{3+}$ crystal along the $C$-axis. The general trend of the theoretically obtained thickness profile of the films is in a good agreement with the experimental values. Furthermore, for a single film, the thickness decreases for relatively larger values of $\theta$ with respect to the normal to the substrate because of a reduction in the particle flux reaching the substrate at such relatively larger angles.


1. B. Toftmann, J. Schou, S. Canulescu. Energy distribution of ions produced by laser ablation of silver in vacuum. *Appl. Surf. Sci.* **278**, 273 (2013).
2. A.A. Voevodin, J.G. Jones, J.S. Zabinski. Characterization of $ZrO_2/Y_2O_3$ laser ablation plasma in vacuum, oxygen, and argon environments. *J. Appl. Phys.* **88**, 1088 (2000).
3. P. Orgiani *et al.* Physical properties of $La_{0.7}Ba_{0.3}MnO_{3-\delta}$ complex oxide thin films grown by pulsed laser deposition technique. *Appl. Phys. Lett.* **96**, 032501 (2010).
4. S.I. Anisimov, D. Bauerle, B.S. Luk'yanchuk. Gas dynamics and film profiles in pulsed-laser deposition of materials. *Phys. Rev. B* **48**, 12076 (1993).
5. R.K. Singh, J. Narayan. Pulsed-laser evaporation technique for deposition of thin films: Physics and theoretical model. *Phys. Rev. B* **41**, 8843 (1990).
6. M.K. Matzen, R.L. Morse. Structure and observable characteristics of laser driven ablation. *Phys. Fluids* **22**, 654 (1979).
7. A.O. Dikovska *et al.* Thin ZnO films produced by pulsed laser deposition. *J. Optoelectron. Adv. M.* **7**, 1329 (2005).
8. B. Cullity. *Elements of X-ray Diffraction* (Addison-Wesley, 1956).
9. J.-H. Kim, S. Lee, H.-S. Im. The effect of different ambient gases, pressures, and substrate temperatures on $TiO_2$ thin films grown on Si(100) by laser ablation technique. *Appl. Phys. A* **69**, 629 (1999).
10. Zhiyun Zhang, Chonggao Bao, Shengqiang Ma, Lili Zhang, Shuzeng Hou. Effects of deposition power and pressure on the crystallinity of Al-doped ZnO thin at glass substrates by low temperature RF magnetron sputtering. *J. Aust. Ceram. Soc.* **48**, 214 (2012).
11. Y. Wang, W. Tang, L. Zhang. Crystalline size effects on texture coefficient, electrical and optical properties of sputter-deposited Ga-doped ZnO thin films. *J. Mater. Sci. Technol.* **31**, 175 (2015).
12. J.A. Rivera Marquez *et al.* Effect of surface morphology of ZnO electrodeposited on photocatalytic oxidation of methylene blue dye. Part I: Analytical study. *Int. J. Electrochem. Sci.* **6**, 4059 (2011).
13. S. Abdul-Jabbar *et al.* Influence of substrate temperature on the structural, optical and electrical properties of CdS thin films deposited by thermal evaporation. *Results in Physics* **3**, 173 (2013).
14. A.T.T. Mostako, A. Khare. Effect of target–substrate distance onto the nanostructured rhodium thin films via PLD technique. *Appl. Nanosci.* **2**, 189 (2012).


Received 05.12.17

*М. Гемечу, Т. Абебе*

СТРУКТУРИ І ПРОФІЛІ ТОНКИХ $KY_3F_10:Ho^{3+}$ ПЛІВОК, НАНЕСЕНИХ ІМПУЛЬСНИМ ЛАЗЕРНИМ ВПЛИВОМ

Р е з ю м е

Тонкі $KY_3F_10:Ho^{3+}$ плівки виготовлені методом імпульсного лазерного напилення із застосуванням Nd-YAG лазе-

ра (266 нм, тривалість імпульсу 10 нс, частота повторення 2 Гц) на 1 см × 1 см підкладку з кремнію в вакуумі для різних відстаней між мішенню і підкладкою. Рентгенівські дослідження показали, що плівки кристалізуються в тетрагональну полікристалічну фазу $KY_3F_{10}$ (відповідно до карти № 27-0465 Комітету з дифракційних стандартів). Наведено результати розрахунків профілів з урахуванням деяких експериментальних параметрів напилення. У припущенні еліпсоїдального поширення струменя плазми, профіль товщини плівки оцінений рішенням газодинамічних рівнянь у разі адіабатичного поширення струменя плазми у вакуумі. Результати дають переважний напрямок пучка вперед, що добре узгоджуються з експериментом. Теорія і експеримент показують зменшення товщини плівки при збільшенні відстані між мішенню і підкладкою, що відповідає зменшенню швидкості напилення. Товщина плівки також зменшується для відносно великих радіальних кутів щодо нормалі до підкладки.